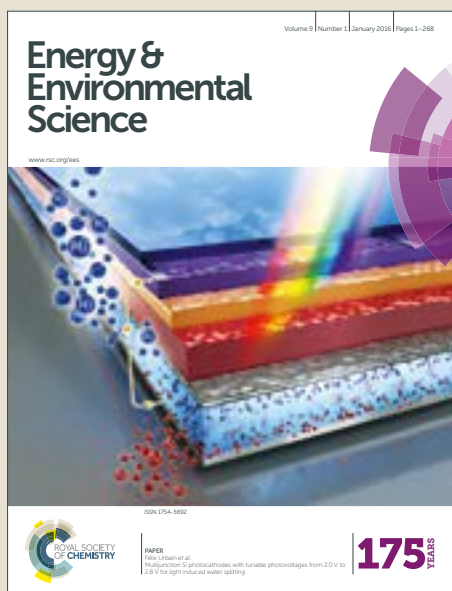


Energy & Environmental Science

Accepted Manuscript



This article can be cited before page numbers have been issued, to do this please use: G. Sievi, D. Geburtig, T. Skeledzik, A. Bösmann, P. Preuster, O. Brummel, F. Waidhas, M. A. Montero, P. Khanipour, I. Katsounaros, J. Libuda, K. Mayrhofer and P. Wasserscheid, *Energy Environ. Sci.*, 2019, DOI: 10.1039/C9EE01324E.



This is an Accepted Manuscript, which has been through the Royal Society of Chemistry peer review process and has been accepted for publication.

Accepted Manuscripts are published online shortly after acceptance, before technical editing, formatting and proof reading. Using this free service, authors can make their results available to the community, in citable form, before we publish the edited article. We will replace this Accepted Manuscript with the edited and formatted Advance Article as soon as it is available.

You can find more information about Accepted Manuscripts in the [author guidelines](#).

Please note that technical editing may introduce minor changes to the text and/or graphics, which may alter content. The journal's standard [Terms & Conditions](#) and the ethical guidelines, outlined in our [author and reviewer resource centre](#), still apply. In no event shall the Royal Society of Chemistry be held responsible for any errors or omissions in this Accepted Manuscript or any consequences arising from the use of any information it contains.

Towards an efficient Liquid Organic Hydrogen Carrier fuel cell concept

View Article Online
DOI: 10.1039/C9EE01324E

Gabriel Sievi,^a Denise Geburtig,^b Tanja Skeledzic,^a Andreas Bösmann,^b Patrick Preuster,^a Olaf Brummel,^c Fabian Waidhas,^c María A. Montero,^d Peyman Khanipour,^a Ioannis Katsounaros,^a Jörg Libuda,^{c,e} Karl J. J. Mayrhofer,^a Peter Wasserscheid^{a,b,e}

- ^a Forschungszentrum Jülich, Helmholtz-Institut Erlangen-Nürnberg für Erneuerbare Energien (IEK 11), Egerlandstrasse 3, 91058 Erlangen, Germany.
- ^b Lehrstuhl für Chemische Reaktionstechnik, Friedrich-Alexander-Universität Erlangen-Nürnberg (FAU), Egerlandstrasse 3, 91058, Erlangen, Germany.
- ^c Lehrstuhl für Physikalische Chemie 2, Friedrich-Alexander-Universität Erlangen-Nürnberg (FAU), Egerlandstrasse 3, 91058, Erlangen, Germany.
- ^d Instituto de Química Aplicada del Litoral, IQAL (UNL-CONICET), Programa de Electroquímica Aplicada e Ingeniería Electroquímica, PRELINE (FIQ-UNL) Santa Fe, Argentina.
- ^e Erlangen Catalysis Resource Center (ECRC), Friedrich-Alexander-Universität Erlangen-Nürnberg (FAU), Egerlandstrasse 3, 91058, Erlangen, Germany.

Contact details of the corresponding author:

Phone: (+49)-(0)9131-85-27420 Fax: (+49)-(0)9131-85-27421; e-mail: peter.wasserscheid@fau.de

AbstractView Article Online
DOI: 10.1039/C9EE01324E

The high temperature required for hydrogen release from Liquid Organic Hydrogen Carrier (LOHC) systems has been considered in the past as the main drawback of this otherwise highly attractive and fully infrastructure-compatible form of chemical hydrogen storage. According to the state-of-the-art, the production of electrical energy from LOHC-bound hydrogen, e.g. from perhydro-dibenzyltoluene (H18-DBT), requires provision of the dehydrogenation enthalpy (e.g. 65 kJ mol⁻¹(H₂) for H18-DBT) at a temperature level of 300 °C followed by purification of the released hydrogen for subsequent fuel cell operation. Here, we demonstrate that a combination of a heterogeneously catalysed transfer hydrogenation from H18-DBT to acetone and fuel cell operation with the resulting 2-propanol as a fuel, allows for an electrification of LOHC-bound hydrogen in high efficiency (> 50 %) and at surprisingly mild conditions (temperatures below 200 °C). Most importantly, our proposed new sequence does not require an external heat input as the transfer hydrogenation from H18-DBT to acetone is almost thermoneutral. In the PEMFC operation with 2-propanol, the endothermal proton release at the anode is compensated by the exothermic formation of water. Ideally the proposed sequence does not form and consume molecular H₂ at any point which adds a very appealing safety feature to this way of producing electricity from LOHC-bound hydrogen, e.g. for applications on mobile platforms.

Keywords

Hydrogen, Liquid Organic Hydrogen Carrier, fuel cell, transfer hydrogenation, 2-propanol

Broader Context

View Article Online
DOI: 10.1039/C9EE01324E

Hydrogen storage in Liquid Organic Hydrogen Carriers (LOHC) enables a new type of hydrogen economy that makes use of the existing infrastructure for liquid fuels. However, this otherwise highly attractive technology has one major drawback: Producing electricity from LOHC-bound hydrogen requires a three step process. First, hydrogen is released from the LOHC in a catalytic dehydrogenation reaction, then the hydrogen is purified, and, finally, the hydrogen is converted to electricity in a fuel cell. Hydrogen release from LOHCs is endothermic and, thus, catalytic dehydrogenation requires high temperatures and constant supply of heat. This limits the overall efficiency of the storage cycle. In our contribution, we propose an alternative and highly promising way to convert LOHC-bound hydrogen into electricity. The hydrogen-rich carrier is unloaded in a thermoneutral transfer hydrogenation and the product of the transfer hydrogenation is directly converted in a fuel cell. Our concept enables conversion of LOHC-bound hydrogen to electricity without external heat input and at very mild conditions. Therefore, the new concept is very attractive for the on-board generation of electric energy in mobile applications.

1. Introduction

View Article Online
DOI: 10.1039/C9EE01324E

Among the chemical energy storage technologies aiming for storing hydrogen in hydrogen-rich solids, liquids or gases, the Liquid Organic Hydrogen Carrier (LOHC) technology is particularly attractive as it allows for hydrogen handling in high volumetric energy storage density under ambient conditions in the infrastructure of today's fuels [1, 2, 3]. LOHC systems consist of pairs of hydrogen-lean, typically aromatic liquids (H0-LOHC), and hydrogen-rich, typically alicyclic liquids (Hx-LOHC). H0-LOHC stores hydrogen in an exothermic catalytic hydrogenation reaction while hydrogen-release from Hx-LOHC compounds proceeds by an endothermic catalytic dehydrogenation reaction.

Among the published LOHC systems, the pair dibenzyltoluene (H0-DBT)/perhydro dibenzyltoluene (H18-DBT) has received special attention [4]. This is due to the fact that H0-DBT is an industrially well-established heat transfer oil since the late 1960s. The substance is characterised by excellent technical availability, attractive cost (2-4 € kg⁻¹ on technical scale), very high thermal stability as well as excellent safety and toxicological properties. The finding that dibenzyltoluene represents an excellent hydrogen storage medium with 6.23 mass % hydrogen capacity (2.05 kWh kg⁻¹) [5] and high cycling stability [6], paved the way to the first commercial applications of this LOHC system [7]. Applications in the field of hydrogen logistics, in particular over longer distances (> 200 km transport distance) [8, 9], represent attractive business cases nowadays.

The production of electricity from LOHC-bound hydrogen, however, has been regarded as less attractive to date. The reason is that the release of elemental hydrogen from the charged carrier molecule is an endothermal process that has to be carried out at high temperatures for thermodynamic reasons. Complete hydrogen release from H18-DBT requires, for example, a temperature of 290 °C at 1.5 bar absolute hydrogen pressure. Moreover, all LOHC systems that do not contain heteroatoms are characterised by a relatively high heat of dehydrogenation, e.g. 65 kJ mol⁻¹ H₂ in the case of perhydro-dibenzyltoluene dehydrogenation [10].

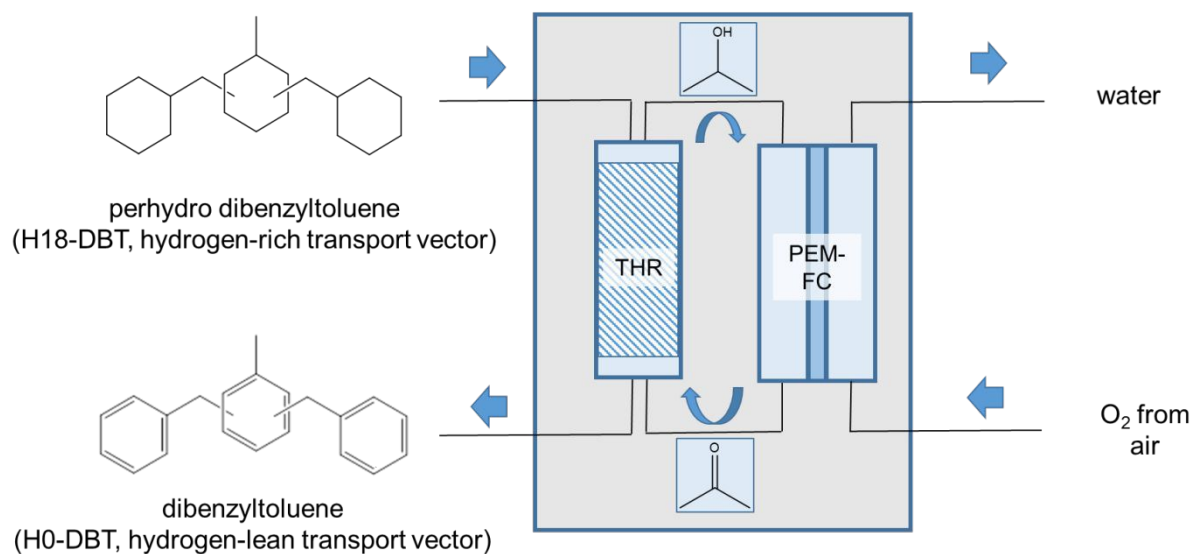
Consequently, publications comparing the pros and cons of different hydrogen storage technologies, have always considered the need for high temperature dehydrogenation processes with significant heat input to drive the endothermal dehydrogenation as the main drawback of storing hydrogen in hydrogen-rich hydrocarbon compounds [11]. In this context, the energetic analysis of the state-of-the-art production of electricity from H18-DBT-bound hydrogen is quite instructive: 27 % of the combustion heat of the LOHC-bound hydrogen has to be invested to fully release the LOHC-bound hydrogen in the form of H₂ gas. Utilisation of the released hydrogen, e.g. in a polymer electrolyte membrane fuel cell (PEMFC) with 50 to 60 % efficiency, results in an overall efficiency from LOHC-bound hydrogen to electricity (in the following abbreviated as BH2E-efficiency) of only 36.5 to 43.8 %. For applications that intend to power a vehicle by LOHC-bound hydrogen, the sequence of hydrogen-release and PEMFC operation is even less efficient if LOHC-released hydrogen is applied to heat the on-board hydrogen

release unit. In such a scenario, the hydrogen used as heating fuel to drive dehydrogenation also has to be released beforehand from the LOHC carrier on-board of the vehicle. This reduces the BH2E-efficiency into the range of 31.5 to 37.8 %.

One obvious way to improve the BH2E-efficiency is heat integration between the endothermal hydrogen-release process and the exothermal fuel cell operation. The feasibility of this approach has been recently demonstrated in the combination of hydrogen release from H18-DBT and Solid Oxide Fuel Cell (SOFC) operation at 650 °C. For this combination, a BH2E-efficiency of 45 % was demonstrated [12]. Unfortunately, the technology readiness level, commercial availability and practicality of SOFCs is to date very limited (at least for applications in the mobility sector and for dynamic applications) so that technical products combining LOHC-release and SOFC operation appear to be out of reach for another couple of years. In contrast, PEMFCs are currently commercially available products that are used for example in hydrogen cars or hydrogen trains [13].

Up until now it has been thought that any form of heat integration between PEMFCs and hydrogen-release from hydrocarbon LOHC-systems would be unfeasible due to the low temperature level of the exothermal fuel cell operation (80 to 180 °C) [14] compared to the high temperature level needed for the endothermal hydrogen release from, e.g. H18-DBT at 280 to 320 °C.

In this contribution, we present a concept that offers an exciting new possibility to circumvent the above-described limitation and offers the potential for converting H18-DBT-bound hydrogen to electricity with a BH2E-efficiency greater than 50 % at a temperature level below 200 °C. In detail, our concept involves a sequence of transfer hydrogenation from H18-DBT to acetone and the direct use of the transfer hydrogenation product 2-propanol as organic fuel in a PEMFC. Our new concept is characterised by the following features: i) The transfer hydrogenation from H18-DBT to acetone is almost thermoneutral and is effective at temperatures below 200 °C leading to a gaseous mixture of 2-propanol and acetone; ii) Condensation of 2-propanol and recycling of acetone-rich vapours back to the transfer hydrogenation unit; iii) evaporation of the 2-propanol-rich mixture for direct PEMFC operation. Our approach aims for the direct PEMFC operation with 2-propanol-rich gaseous feed and air as feed streams and formation of electricity, water and acetone as the sole products. The formation of CO₂ or other organic decomposition products must be avoided in order to close the transfer hydrogenation/electrification cycle as shown in Scheme 1.



Scheme 1: Conversion of H18-DBT-bound hydrogen to electricity in a sequence of transfer hydrogenation of acetone to 2-propanol in the transfer hydrogenation reactor (THR) followed by use of the formed 2-propanol as organic fuel in a subsequent PEM fuel cell. Acetone produced in the fuel cell is recycled and undergoes another cycle of transfer hydrogenation and electrification.

Why is the 2-propanol/acetone reaction pair a particularly suitable hydrogen transfer medium for our concept? The use of 2-propanol as fuel for PEMFCs has already been described in the literature [15, 16, 17]. In these contributions, it has been shown that fuel cell operation with 2-propanol allows for high open circuit voltage. It has been claimed that the main electrooxidation product of 2-propanol is acetone due to the fact that the C-C bond of the secondary alcohol is hard to cleave [18]. Yet, it has been stated that oxidation of 2-propanol only transforms one mole of chemically bound hydrogen per 2-propanol to protons in a 2-electron process (corresponding to a gravimetric hydrogen capacity of 3.3 %) and this fact has been considered as a main disadvantage of the system [19].

In our concept, however, this remarkable stability of acetone against further oxidation offers the opportunity for an emission-free fuel cell without supply of molecular hydrogen, if a 2-propanol-operated fuel cell is combined with an effective transfer hydrogenation from the excellent hydrogen transport/storage molecule H18-DBT. Herein, acetone is activated in the transfer hydrogenation reaction and serves as recyclable transfer medium in our intended process. Thus, the stability of the 2-propanol/acetone couple under fuel cell operation conditions is of great advantage for our concept, while the low energy density deficiency of the partial reduction in only a 2-electron process becomes negligible in the recycling operation strategy. Moreover, acetone and 2-propanol are cheap and technically available chemicals with benign ecotoxicological properties. Both compounds enable a PEMFC operation at 85 °C with gaseous reactants due to their low boiling points.

Our concept offers a number of very intriguing features for many practical applications: i) the process at no point produces elemental hydrogen but only organic molecules and protons, thus offering attractive perspectives with regard to safety aspects of the resulting power device, e.g. for mobile applications; ii) the overall process does not require the input of external heat flows; while the heat of H18-DBT dehydrogenation (+65 kJ mol⁻¹ H₂) [2] matches almost perfectly the heat of acetone hydrogenation (-70 kJ mol⁻¹ H₂) (see calculation in the ESI), the fuel cell operation with the 2-propanol feed is an overall exothermal process; iii) in contrast to direct methanol fuel cells [20] the 2-propanol fuel cell applied here does not produce any CO₂ emissions; iv) in contrast to literature-known direct LOHC fuel cell concepts based on N-containing LOHC-systems [21, 22], the approach proposed here does not show incompatibilities between the acidic ionomer and basic LOHC compounds.

This paper reports on our recent scientific and technological developments to bring this concept closer to realisation for off-grid power devices or for energy production on mobile platforms. The paper focuses on the transfer hydrogenation of H18-DBT with acetone and investigates PEMFC operation with acetone/2-propanol mixtures. Moreover, we study 2-propanol electrokinetics and selectivity at PtRu/C-anodes in comparison to pure Pt/C-anodes. We also calculate the potential efficiency of the proposed sequence and pinpoint aspects that deserve further development to fully leverage the technical potential of the proposed concept.

2. Experimental

Transfer hydrogenation of acetone to 2-propanol with H18-DBT as hydrogen source

All transfer hydrogenation experiments were performed by using a 500 mL stainless steel Parr batch autoclave equipped with a four-blade gas-entrainment stirrer ($n = 1000$ rpm). To assure an inert atmosphere in the pressure vessel, the reactor was purged with argon three times. The reactor was heated to the desired reaction temperature with an external electrical heating jacket. To determine the progress of the reaction, liquid samples were taken and analysed by gas chromatography (Varian 3900 equipped with a CP Sil PONA CB50 m x 0.21 mm capillary column). As catalyst, Pt on carbon with a metal content of 0.25 mol % with respect to the applied H18-DBT and acetone was used. The initial ratio of H18-DBT to acetone was 1.

Fuel cell studies with hydrogen, 2-propanol and 2-propanol/acetone mixtures

The fuel cell measurements were performed in a fuel cell system from balticFuelCells GmbH (qCf FC25/100 V1.1 [23]) at 85 °C, slightly above the boiling point of 2-propanol of 82 °C. On the cathode side, pressurised air was saturated with distilled water at 85 °C and fed to the cell with 1 L_N min⁻¹. On the anode side, 50 g h⁻¹ of the various 2-propanol/acetone fuel mixtures were evaporated and then fed to the cell using N₂ as carrier gas (also 1 L_N min⁻¹ and saturated with water at 85 °C as on the cathode side). For the experiments with other fuels, 0.2 L_N min⁻¹ hydrogen or 50 g h⁻¹ methanol were used. As

membrane electrode assembly (MEA), a direct methanol fuel cell (DMFC) MEA from Alfa Aesar with a Nafion® 115 membrane (active surface = 25 cm²) and nominal Pt loadings of 2.7 and 2.0 mg cm⁻² on the anode and cathode sides respectively, were used. The anode side had an additional nominal Ru loading of 1.3 mg cm⁻². A Sigracet® GDL 10BC was added as additional gas diffusion layer and for improved mechanical stability. An electronic load from dhs tools GmbH PLZ664WA was applied.

Prior to each measurement, the cell was conditioned with a hydrogen flow of 0.2 L_N min⁻¹ during the heating phase for reduction of the active centres. The cell was held at OCP under fuel atmosphere until it was saturated and stable. While recording the current density-voltage-curve (j-U-curve) the voltage at each stage was kept constant for 10 minutes (constant voltage, CV mode) starting at OCP and decreasing the voltage stepwise (50 mV) down to 100 mV. The plotted current data are the mean values of each increment (minutes 2 to 10).

Stack measurements were carried out in a stack from ElectroChem. The measuring conditions are the same as for the single cell measurements. The applied stack consisted of 20 cells, each one with an active area of 50 cm². The stack was cooled between each two MEAs. The baseline experiment with only hydrogen as the fuel used 2 L_N min⁻¹ hydrogen (saturated at 85 °C with water for anode wetting) as anode feed and 5 L_N min⁻¹ pressurised air at the cathode. All gases were electrically heated (85 °C) and the stack temperature of 85 °C was controlled by a Huber Unistat T305 with a mixture of deionised (90 %) and tap (10 %) water. For the pure 2-propanol baseline experiment, a 114 g h⁻¹ azeotropic 2-propanol/water mixture (87.6 wt. % 2-propanol = 100 g h⁻¹) and 1.5 L_N min⁻¹ pressurised wet air were used at the anode and cathode, respectively. In addition, 0.5 L_N min⁻¹ nitrogen was used as a carrier gas at the anode. For the fuel cell experiments with 2-propanol/acetone mixtures, the procedure was the same as with the azeotropic 2-propanol/water mixture, however, the fuel feed contained 70 g h⁻¹ 2-propanol, 30 g h⁻¹ acetone and 14 g h⁻¹ deionised water. The A fuel mixture consisting of 30 g h⁻¹ methanol and 30 g h⁻¹ deionised water was used for the methanol stack experiment.

Electrochemical Real-time Mass Spectrometry (EC-RTMS)

For EC-RTMS measurements, the electrolyte was 0.1 M HClO₄ + 0.2 M 2-propanol. The working electrode was carbon-supported nanoparticles (Alfa Aesar, Pt : Ru 40 : 20 wt. % on carbon black, HiSPEC® 10000 and Pt 40 wt. % on carbon black, HiSPEC® 4000) with a loading of 30 μg_{Pt} cm⁻² deposited on a glassy carbon substrate. Although a Ag/AgCl reference electrode and a carbon counter electrode were used, the potential is always expressed on a reversible hydrogen electrode (RHE) scale, calibrated via the open circuit potential of platinum in a 2-propanol-free, hydrogen-saturated solution. A scanning flow cell (SFC) with an inlet flow rate of 0.5 mL min⁻¹ was used for the electrochemical measurements. A thin capillary channel (520 μm ID) was positioned on top of the working electrode to withdraw the electrolyte for analysis (0.4 mL min⁻¹) while an additional waste channel (0.1 mL min⁻¹) was utilised as in the classical SFC configuration [24]. Chronoamperometric experiments were

performed by applying a certain potential in the range of 0.05 to 0.5 V_{RHE} for 5 minutes. A 3-minute step at 0 V always preceded each measurement to remove the previously adsorbed acetone from the catalyst surface. During every electrochemical measurement, the withdrawn electrolyte was analysed in real-time with a direct analysis in real time (DART) mass spectrometer and a time-of-flight mass analyser (AccuTOF™-DART® 4G from JEOL) equipped with a DART ion source (IonSense Inc) after being nebulised with an argon stream (0.3 L min^{-1}). Acetone was detected by integration of the mass spectrum in the m/z range 59.0 to 59.2 amu, which corresponds to the $\text{CH}_3\text{COCH}_3\text{-H}^+$ ion. The frequency of data acquisition was 1 Hz, the temperature of the ion source was 300 °C and the orifice voltage was 30 V. CO_2 was extracted from the liquid phase with a hydrophobic Teflon membrane positioned at the cell outlet. The extracted CO_2 molecules were ionised with an electron ionisation source, analysed with a quadrupole mass analyser and detected with a secondary electron multiplier detector (Extrel MAX300-LG). Details on the EC-RTMS method can be found in [25].

Electrochemical Infrared Reflection Absorption Spectroscopy (EC-IRRAS)

Prior to our EC-IRRAS measurements, all glass and Teflon equipment as well as all noble metal wires were stored in a solution of NOCHROMIX (Sigma Aldrich) and concentrated sulphuric acid (Merck, Emsure, 98 %) overnight. Before starting the experiments, all equipment was rinsed 5 times with ultra-pure (MilliQ Synergy UV, 18.2 $\text{M}\Omega\cdot\text{cm}$ at 25 °C, TOC < 5ppm) and, subsequently, boiled 3 times in Milli-Q water for at least 15 min. All noble metal wires were annealed in the flame of the Bunsen burner and afterwards rinsed with ultra-pure water.

For the EC-IRRAS measurements, the nanoparticles (same as above for EC-RTMS) were first dispersed in ultra-pure water, subsequently deposited on a head shaped polycrystalline Au crystal (Safina, 99.99 %, 110 mm^2) and, finally, dried under N_2 flow. In order to guarantee a clean sample surface, the working electrode (WE) was cycled 5 times between 0.05 and 1.1 V_{RHE} with a scan rate of 50 mV s^{-1} before each measurement. The voltammograms were recorded in a 0.1 M HClO_4 (Merck, Suprapur®) solution in a separate cell and under inert atmosphere. The potential was controlled using a Gamry Reference 600+ potentiostat. All measurements were performed in a three electrode configuration using an Au wire (Hauner, 99.999 %) as counter (CE) and a homebuilt RHE as reference electrode (RE). The potential control was maintained during the whole measurement.

The infrared spectra were measured with a vacuum-based IR spectrometer (Bruker Vertex 80v) with evacuated optics for electrochemical measurements, a homebuilt electrochemical cell, and a liquid nitrogen cooled HgCdTe (MCT) detector. A CaF_2 hemisphere (Korth, \varnothing 25 mm) was used as IR transparent window material. The background spectra were recorded at 0.05 V_{RHE} with 256 scans per spectrum before each measurement. Potential dependent spectra were measured by stepwise increase of the potential (0.1 V) between 0.05 and 0.5 V_{RHE} with 128 scans per spectrum with a resulting acquisition time of 57 s and a resolution of 2 cm^{-1} . All IR measurements were performed in a degassed (Ar 5.0,

Linde, > 50 cc min⁻¹) solution of 0.2 M 2-propanol (Sigma Aldrich, electronic grade, 99.999 %) in 0.1 M HClO₄. Attenuated total reflectance (ATR) reference measurements were acquired using a Ge window in the same setup.

Results and Discussion

Transfer hydrogenation of acetone to 2-propanol using H18-DBT-bound hydrogen

The transfer hydrogenation from H18-DBT to acetone serves in the here-pursued concept as the first step to activate the hydrogen from H18-DBT. The second step utilises the 2-propanol formed as fuel for the PEMFC operation. In order to validate the selective 2-propanol formation from H18-DBT and acetone, we first performed batch autoclave experiments at different reaction temperatures with Pt on carbon as the catalyst. We aimed for performing the transfer hydrogenation at temperatures as mild as possible in order to reduce the temperature level of the entire process (LOHC-bound hydrogen to electric power) for enhanced system dynamics. The results of these experiments are shown in Figure 1.

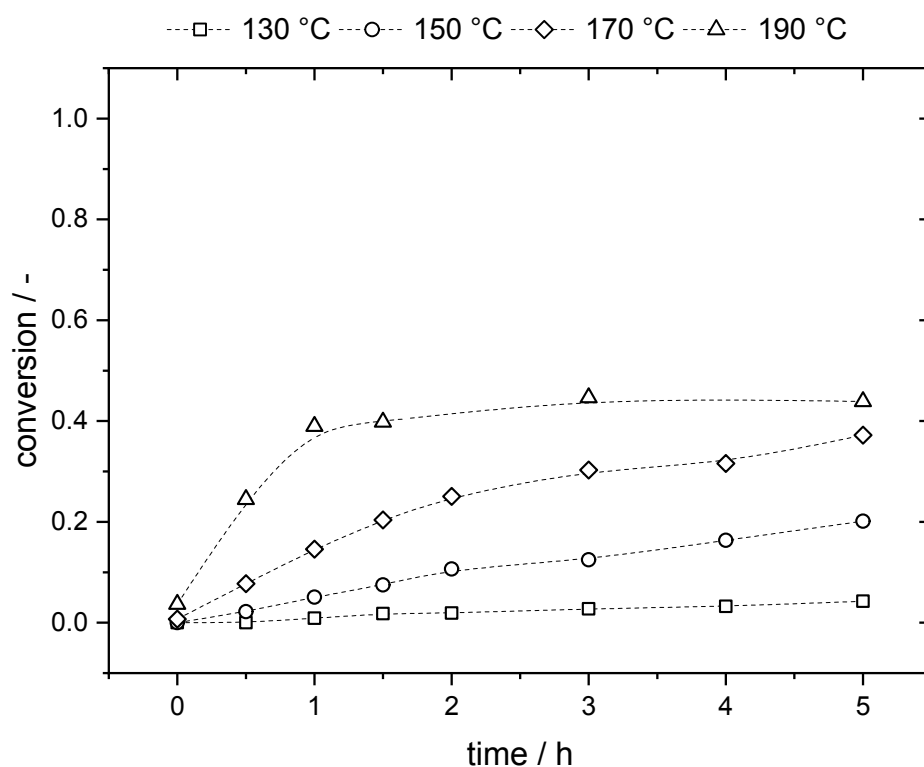


Figure 1: Conversion of acetone in the transfer hydrogenation of acetone with LOHC-bound hydrogen using platinum on carbon (5 wt. %) as catalyst; reaction conditions: LOHC = H18-DBT; H18-DBT : acetone = 1 : 1; acetone : Pt = 400 : 1; depending on the temperature level, a pressure in the autoclave between 6 bar (130 °C) and 13 bar (190 °C) established by partial evaporation of the acetone/2-propanol mixture.

Surprisingly, a temperature of 190 °C proved enough to reach the transfer hydrogenation equilibrium within 2 h. Under these conditions 2-propanol was the only detectable product in the reaction mixture and an equilibrium yield of 45 % in 2-propanol was established in the reactor. Analysis of the H18-DBT hydrogen donor revealed after the experiment the expected degree of dehydrogenation. Note, that one mole of H18-DBT can provide 9 moles of hydrogen. Consequently, for the applied ratio of H18-DBT to acetone of 1, the formation of 45 % 2-propanol corresponds to a reduction of the degree of hydrogenation in the hydrogen donor of around 5 %. Even lower temperatures can be applied and enable acetone conversion, however, at significantly reduced rates. At a temperature of 130 °C the reaction becomes very slow with the applied, non-optimised Pt on carbon catalyst.

Still, these results prove that the hydrogen release from H18-DBT proceeds at much milder conditions if the hydrogen is utilised immediately for the hydrogenation of acetone instead of the formation of elemental hydrogen, which would require at least 250 °C to proceed to any appreciable extent with the here-applied Pt on carbon catalyst. It is also noteworthy that in batch experiments with a high H18-DBT : acetone ratio of 2, the equilibrium of the transfer hydrogenation shifted to 58 %.

To further approach the reaction conditions suggested by our overall hydrogen activation concept highlighted in Scheme 1, we also performed a semi-continuous version of the transfer hydrogenation experiment at ambient pressure conditions (see ESI for details). For this purpose we filled a vertical stainless steel tubular reactor ($V_{\text{tube}} = 650$ ml) with 200 g of a spherical Pt/AlO_x catalyst (Pt-loading = 0.3 wt.%, alumina pellets were chosen as catalyst support in this experiment to limit the pressure drop, note that the use of the alumina support is not ideal as this support induces some aldol side reactions) and 393 ml of H18-DBT. At 170 °C, 100 ml/min acetone vapour was fed to the reactor in a bubble column operation mode resulting in a hydrodynamic residence time of 3.93 min. Under these conditions a 2-propanol yield of 13.6 % established at the reactor exit in quasi steady-state operation after 1 h operation time. This non-optimised experiment proves in principle that the acetone transfer hydrogenation to 2-propanol is feasible at ambient pressure and with continuous acetone feeding. We anticipate that increasing the residence time and optimizing the catalyst support will help to approach equilibrium conversion at minimal side product formation also for continuous acetone feeding. Such studies are currently underway in our laboratories.

From these results we conclude that the transfer hydrogenation device should be operated in a counter-current mode, i.e. with almost pure acetone vapour entering the bottom side of the reactor and bubbling through the catalyst bed that is fully wetted with the LOHC carrier that should flow in counter-current. Applying a suitable residence time, the LOHC-material has already transferred most of its hydrogen at the bottom of the vertical hydrogen transfer reactor. At the top of the reactor, in contrast, the 2-propanol-rich vapour is contacted in counter-current with pure H18-DBT to drive the transfer hydrogenation reaction to the highest possible 2-propanol yields.

Of course, there is always the possibility of producing an even more enriched 2-propanol fuel cell feed. Taking benefit from the boiling point difference between 2-propanol (bp = 82 °C) and acetone (bp = 56 °C) and the fact that the acetone/2-propanol system does not form an azeotrope, selective condensation of 2-propanol at 70 °C is a suitable way of 2-propanol/acetone separation. The energy for the subsequent re-evaporation of the condensed 2-propanol to feed the fuel cell with a gaseous fuel can be provided by using waste heat from the fuel cell operation at 85 to 90 °C. It is also noteworthy that both 2-propanol and acetone form a pronounced miscibility gap with the applied LOHC system in the whole range from H0-DBT to H18-DBT. Therefore, cross-contamination of the LOHC-system with 2-propanol/acetone in the effluent of the transfer hydrogenation reactor is not a major issue as liquid-liquid separation in a subsequent separator unit is easily achieved. Contamination of the LOHC-system in 2-propanol/acetone is not a problem due to the very large boiling point difference and the fact that the 2-propanol/acetone mixture is entering the fuel cell in form of vapour.

2-Propanol and 2-propanol-acetone as fuels for the PEMFC

As shown above, the transfer hydrogenation of acetone with H18-DBT produces 2-propanol/acetone equilibrium mixtures. The composition of the latter depends on the LOHC/acetone ratio, reaction temperature and pressure, but also on the eventual use of 2-propanol/acetone separation units between the transfer hydrogenation unit and the fuel cell. In order to evaluate the best operation strategy, the fuel cell performance with different 2-propanol/acetone mixtures was investigated in a single cell electrochemical set-up. A commercial direct methanol fuel cell (DMFC) MEA containing a PtRu/C anode was utilised for this purpose without dedicated optimisation for the specific application of a 2-propanol/acetone fuel.

Figure 2a shows the current density-voltage-curves of different 2-propanol/acetone fuel mixtures ranging from 0 to 100 % 2-propanol. Figure 2b presents the corresponding power densities.

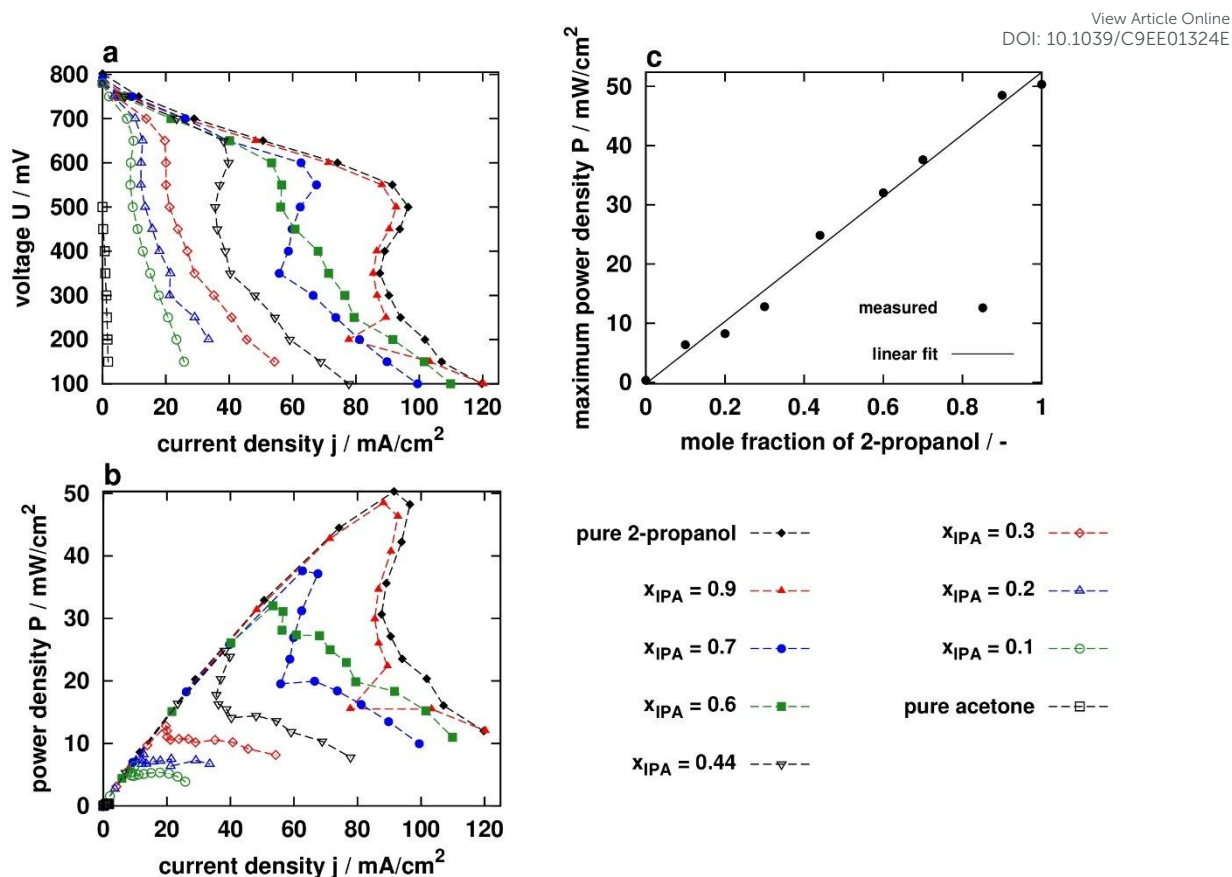


Figure 2: Current density-voltage (a) and power density-current-density (b)-curves of different 2-propanol/acetone mixtures. c) maximum power density depending on the mole fraction of 2-propanol in a mixture of 2-propanol and acetone. Conditions: $T = 85\text{ }^{\circ}\text{C}$, 50 g h^{-1} 2-propanol/acetone, $1\text{ L}_\text{N}\text{ min}^{-1}$ nitrogen, $1\text{ L}_\text{N}\text{ min}^{-1}$ pressurised air. Material: DMFC-MEA (5-layer, PtRu/C anode).

With pure 2-propanol as fuel, our set-up shows an OCP of 802 mV. Under current flow the maximum power density of 50.4 mW cm^{-2} is achieved at a voltage of 550 mV. The use of PtRu/C as anode catalyst is decisive for the observed performance with the 2-propanol fuel. The appearance of a maximum current density in Figure 2a at 550 mV is not related to mass transport limitations, but it is an intrinsic characteristic of the PtRu catalyst (see ESI, Figure S2). In comparison, pure Pt as the anode led to an OCP of only $\sim 670\text{ mV}$ and a maximum power density of 3.6 mW cm^{-2} at 200 mV (see ESI, Figure S3).

As shown in Figure 2c, the maximum power density shows a linear increase with the amount of 2-propanol in the mixture, from no power density when the fuel cell is fed with inactive acetone, to achieving a maximum power density when pure 2-propanol is used. Table 1 shows some characteristic data of the fuel cell measurements, including the OCP, the maximum power density and the efficiencies of the fuel cell. It is highly remarkable that the efficiency of converting 2-propanol-bound hydrogen to electricity is as high as 59%. Combined with the thermoneutral transfer hydrogenation, an optimised process of the transfer hydrogenation/fuel cell sequence offers therefore the potential of BH₂E-efficiencies well above 50%. Note, that from a thermodynamic point of view, the maximum efficiency of a fuel cell process with 2-propanol as fuel is 98% (see ESI for details).

Table 1: Characteristic data from the current-voltage-curves of different 2-propanol/acetone fuel mixtures. View Article Online
DOI: 10.1039/C9EE01324E

X _{2-propanol} (-)	1	0.9	0.7	0.6	0.44	0.3	0.2	0.1
OCP (mV)	802	786	791	780	780	780	780	780
P _{max} (mW cm ⁻²)	50.4	48.7	37.7	32.1	24.6	12.8	8.2	6.4
η_U (%)	49.9	49.9	54.4	54.4	59.0	59.0	59.0	59.0

For a proper evaluation of the single-cell measurements, we used the same setup (i.e. same cell and MEA) with other, well established fuels (hydrogen or methanol) and the corresponding current-voltage and current-power curves are displayed in Figure 3. Clearly, the performance with the 2-propanol fuel is by a factor of three to four below that of hydrogen (maximum power densities of 170.6 mW cm⁻² for dry and 251.1 mW cm⁻² for water-saturated hydrogen) but significantly better than with the methanol feed, despite the fact that the MEA used had been optimised for the use of methanol as fuel. In particular, the OCP with methanol was significantly lower (479 mV) in accordance with literature [26], and a voltage drop similar to that of 2-propanol led to a current density of ~ 120 mA cm⁻² and a maximum power density of 16.1 mW cm⁻². Considering that the maximum power densities achieved here for hydrogen and methanol are lower than what is possible with state-of-the art material and optimised setups (up to 1 W cm⁻² for hydrogen and 110 mW cm⁻² for methanol [26]), it is expected that there is plenty of room for improving the performance of 2-propanol after proper optimisation. Note, that the relatively low power densities obtained with our fuel cell using dry or wet hydrogen are due to the fact that air at ambient pressure has been used at the cathode (instead of compressed air or pure oxygen) and that the applied MEA has not been designed for an optimal use with hydrogen. The applied membrane and the cathode catalyst layer were too thick to enable operation at high power densities with hydrogen as a fuel. These power density reducing effects are well in-line with literature reports [27, 28].

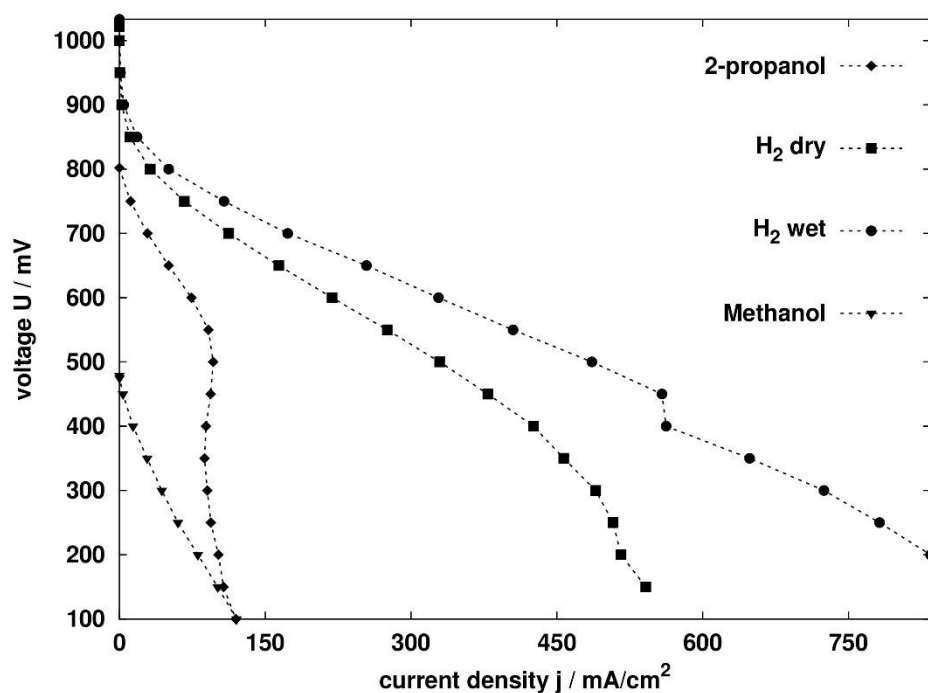


Figure 3: Current-voltage curves of different fuels (2-propanol, methanol, hydrogen (dry and wet)) with the same MEA. Conditions: $T = 85\text{ }^{\circ}\text{C}$, 50 g h^{-1} 2-propanol/acetone, 50 g h^{-1} MeOH, $1\text{ L}_N\text{ min}^{-1}$ nitrogen, $1\text{ L}_N\text{ min}^{-1}$ pressurised air, $0.2\text{ L}_N\text{ min}^{-1}$ hydrogen. Material: DMFC-MEA (5-layer, PtRu/C anode).

Operating a fuel cell stack (20 cells) with 2-propanol and 2-propanol/acetone mixtures

To evaluate the fuel cell performance on larger scale, a commercial DMFC stack with 20 cells (anode catalyst: PtRu/C, ElectroChem) was operated with 2-propanol and the performance was compared to the conversion of hydrogen in the same stack. The current-voltage- and current-power-curves are shown in Figure 4.

The fuel cell stack which was fed with 2-propanol led to an OCP of 15.56 V, corresponding to an OCP per cell of 778 mV. The latter value is in good agreement with our single cell measurements, where an OCP of 802 mV was obtained. With regard to power output, the 2-propanol fuel resulted in 25.3 W at 11 V. This limiting current corresponds to a 55% conversion of 2-propanol to acetone as the sole product. The realised power density in the stack was 25.3 mW cm^{-2} .

The same fuel cell stack with hydrogen as fuel on the contrary was characterised by an OCP of 19.85 V, as expected from the single cell OCP ($\sim 1\text{ V}$) and the number of cells. The maximum power output of the stack with hydrogen was 128.7 W, which is a factor of five more than that with the 2-propanol fuel. This value was achieved at 10 V, corresponding to a maximum power density of 128.7 mW cm^{-2} . The j - U -curve decreases at a current of 15 A in the mass transport regime. At this point full conversion of

the hydrogen feed was observed. An experiment in the same stack with a 2-propanol/acetone mixture with 70 mol % 2-propanol led to an OCP of 15.75 V and a maximum power output of 11.8 W.

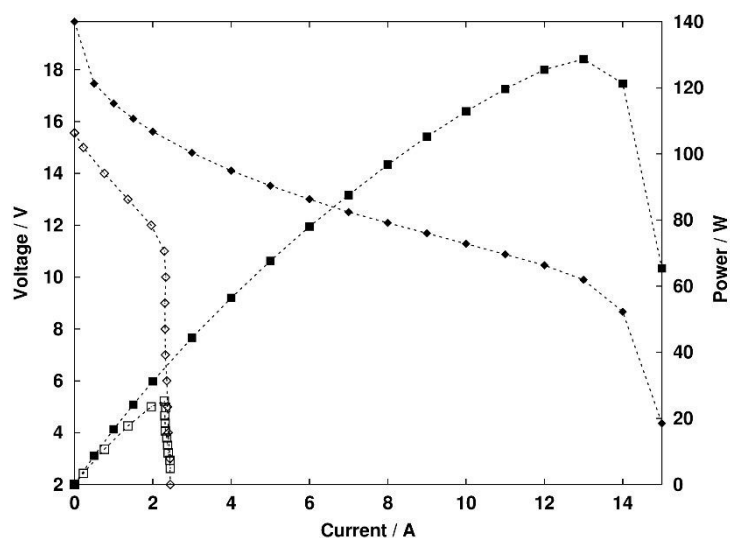


Figure 4: Current-voltage (♦) and current-power (■) curves of 2-propanol (empty symbols) and hydrogen (filled symbols) in a 20 cell stack. Conditions: $T = 85\text{ }^{\circ}\text{C}$, 114 g h^{-1} 2-propanol/water, $0.5\text{ L}_N\text{ min}^{-1}$ nitrogen, 1.5 (for 2-propanol) or 5 (for hydrogen) $\text{L}_N\text{ min}^{-1}$ pressurised air, $2\text{ L}_N\text{ min}^{-1}$ hydrogen. Material: 20 cell stack from ElectroChem with liquid water cooling (alternating sequence of cooling modules and electrochemical cells), DMFC-MEAs (5-layer, PtRu/C anode).

For experiments using methanol as fuel in the same stack, the current density-voltage and current-power curves of 2-propanol and methanol are drawn for comparison purposes in a magnified manner in Figure 5. The OCP of methanol is 12 V , which is significantly lower than for 2-propanol and leads to an overall lower efficiency. At 6 V the maximum power of 15.9 W is reached, which is around 10 W below the value of pure 2-propanol and only slightly above the 70% 2-propanol/ 30% acetone mixture. However, for methanol no characteristic limiting current and mass transport regime is observed. The maximum current of $\sim 4\text{ A}$ was achieved at 2 V , which corresponds to a methanol conversion of 53% . This result is well in-line with the single cell experiments described above.

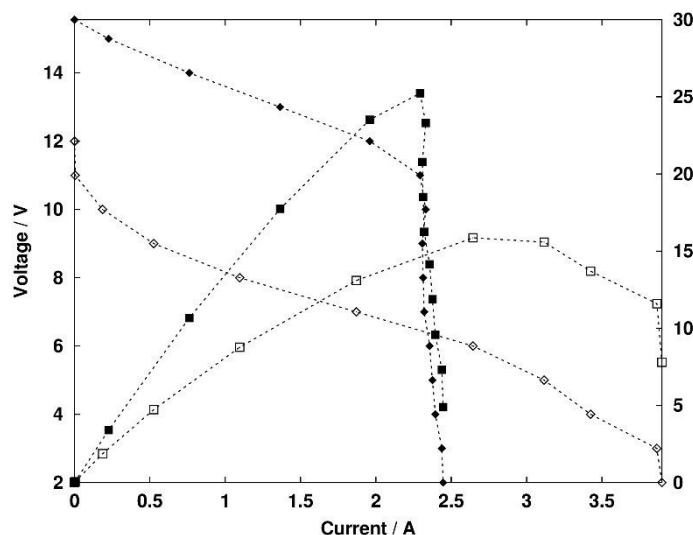


Figure 5: Current-voltage (♦) and current-power (■) curves of 2-propanol (filled symbols) and methanol (empty symbols) in a 20 cell stack. Conditions: $T = 85\text{ }^{\circ}\text{C}$, 114 g h^{-1} 2-propanol/water, 30 g h^{-1} methanol/water, $0.5\text{ L}_N\text{ min}^{-1}$ nitrogen, 1.5 (for 2-propanol) or 2.65 (for methanol) $\text{L}_N\text{ min}^{-1}$ pressurised air, Material: 20 cell stack from ElectroChem with liquid water cooling (alternating sequence of cooling modules and electrochemical cells), DMFC-MEAs (5-layer, PtRu/C anode).

Given the fact that a commercial DMFC stack was utilised without any specific optimisation for 2-propanol as a fuel, we consider these results as very promising. While the stack performance is better with hydrogen, only the use of the 2-propanol fuel allows the operation of the sequence from LOHC-bound hydrogen to electricity without investing the heat of dehydrogenation that would be inevitably required if molecular hydrogen is released from the LOHC storage medium in the first place. At the current state of development, this obvious advantage comes at the price of a less power-dense fuel cell operation. However, we are convinced that further optimisation of the 2-propanol and 2-propanol/acetone fuel cell operation with respect to electrocatalyst and cell design can reduce this disadvantage at a higher level of development.

Development potential of our concept

While the demonstration of the cascade reactions from LOHC-bound hydrogen to electric power has been highly successful, our work also revealed the major challenges that need to be addressed for further optimisation, particularly in relation to the 2-propanol fuel cell performance. In order to identify the key parameters for technological advancement, we performed additional fundamental investigations to understand the essential electrocatalytic anode reaction of 2-propanol in more detail. Specifically, we employed advanced electrochemical real-time mass spectrometry (EC-RTMS, Figures 6a and 6b) and electrochemical infrared reflection-absorption spectroscopy (EC-IRRAS, Figures 6c and 6d) to compare the performance of Pt/C and PtRu/C nanoparticles in electrocatalytic 2-propanol oxidation. These methods provide unique insights into reaction products and species adsorbed at the electrode or present

in the measurement cell. Quantitation is not trivial with any of the two methods, therefore the intensities in figure 6 appear dimensionless. It could be resolved that neither CO₂, CO nor other degradation fragments of 2-propanol or acetone are produced in the relevant potential range up to 0.5 V_{RHE} on both Pt/C and PtRu/C. Combined with the highly selective transfer hydrogenation reaction forming 2-propanol from acetone, this substantiates our claim of a highly effective role of the 2-propanol/acetone reaction pair as hydrogen transfer medium in the here-presented coupled fuel cell operation.

Moreover, we compare the performance of Pt/C and PtRu/C as anode electrocatalysts in the 2-propanol conversion: the onset for acetone formation on Pt/C is at +0.3 V_{RHE}, as evidenced by the small increase of the acetone signal (Figure 6a). This is corroborated by the appearance of negative bands at 1699, 1441, 1427, 1372, and 1240 cm⁻¹ which can be assigned to the $\nu(\text{C}=\text{O})$ (1699 cm⁻¹), $\delta(\text{CH}_3)$ (1441, 1427 cm⁻¹), $\delta_{\text{sym}}(\text{CH}_3)/\nu_{\text{asym}}(\text{C}-\text{C})$ (1372 cm⁻¹), and $\nu_{\text{asym}}(\text{C}-\text{C})$ (1240 cm⁻¹) vibrations of the acetone formed [29] and by positive bands at 1468, 1387, 1308, 1167, 1130 cm⁻¹, which can be assigned to the $\delta_{\text{asym}}(\text{CH}_3)/\delta_{\text{sym}}(\text{CH}_3)$ (1468 cm⁻¹), $\nu(\text{C}-\text{C})$ (1387 cm⁻¹), $\delta(\text{O}-\text{H})$ (1308 cm⁻¹), $\nu(\text{C}-\text{C})$ (1167 cm⁻¹), and $\nu(\text{C}-\text{O})$ (1130 cm⁻¹) modes of the 2-propanol that is consumed [30] (Figure 6c). Note, that negative and positive bands correspond to species that are formed and consumed, respectively. At more positive potentials the acetone-characteristic intensities increase both in EC-RTMS and EC-IRRAS and point as expected at higher reaction rates. A rapid decay of the acetone signal at constant potential in EC-RTMS however, indicates significant poisoning of the Pt/C electrode. As a result, only approximately 20 % of the initial acetone production rate is maintained after 5 minutes at +0.5 V_{RHE} (Figure 6a) with this catalyst. A comparison of infrared spectra measured in p- and in s-polarisation on Pt(111) at +0.5 V_{RHE} show that 2-propanol oxidation is associated with the accumulation of adsorbed acetone (see Supporting Information). Therefore, we attribute the rapid decay of the acetone signal to an increase in the surface coverage of acetone, which blocks active surface sites and hinders further oxidation of 2-propanol. Contrary to Pt/C, 2-propanol oxidation starts already at remarkable ca. +0.1 V_{RHE} on PtRu/C, i.e. very close to the thermodynamic equilibrium potential for the acetone/2-propanol redox couple (+0.13 V at standard conditions, see ESI), and 200 mV lower than the onset observed for Pt/C. The less positive onset potential for 2-propanol oxidation on PtRu/C compared to Pt/C explains the higher OCV value observed for the fuel cell utilizing PtRu/C as the anode. Furthermore, the decay of the acetone signal with time is less pronounced, i.e. ca. 70% of the reaction rate is maintained after 5 minutes at +0.5 V_{RHE}, indicating that acetone poisoning is less severe for PtRu/C. Still, the kinetics for 2-propanol oxidation must be enhanced to enable minimum potential losses and thus maximum power output by increasing the current density. In this direction, the fact that the 2-propanol oxidation is not limited by adsorbed CO implies that the catalyst requirements for 2-propanol oxidation are different than those for the oxidation of primary alcohols such as methanol. This opens up new opportunities for finding catalyst compositions which enhance the crucial desorption of acetone from the surface and thereby enable even more facile kinetics close to the ideal kinetics of hydrogen oxidation.

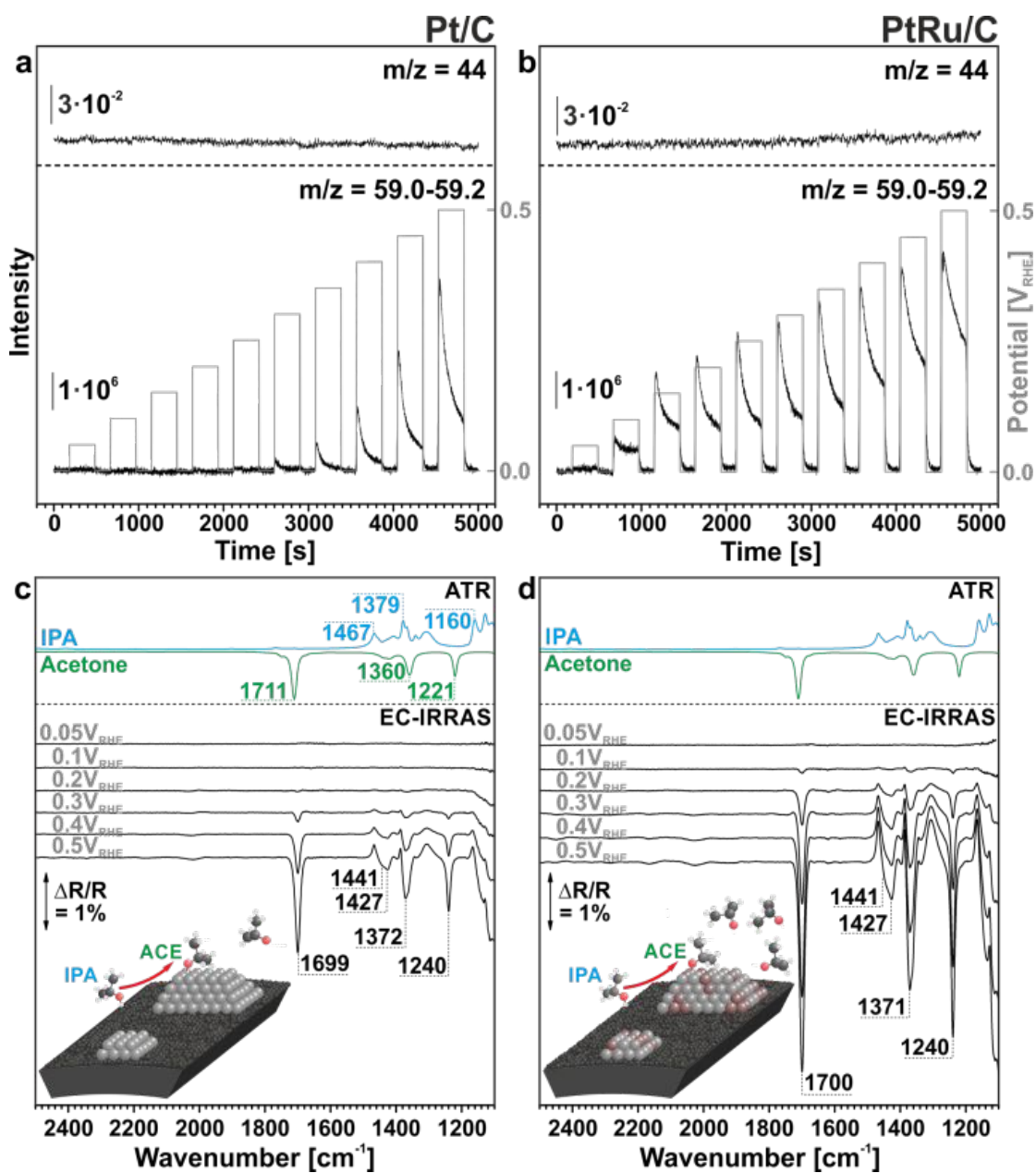


Figure 6: Product formation during the electrochemical 2-propanol oxidation on (a,c) Pt/C and (b,d) PtRu/C, monitored by (a,b) EC-RTMS or (c,d) EC-IRRAS. The reference spectra in EC-IRRAS were acquired at +0.05 V_{RHE}.

Conclusions

View Article Online
DOI: 10.1039/C9EE01324E

Our contribution reports a novel and highly promising way to produce electric power from hydrogen bound to Liquid Hydrogen Storage Carrier (LOHC) compounds. In particular, the production of electric power from H18-DBT in an efficient, low temperature process is described. H18-DBT is an energy-dense (6.23 mass % hydrogen), safe (benign toxicity properties), cost efficient (2 to 4 € kg⁻¹ on industrial scale) and fully infrastructure compatible hydrogen carrier. The here-proposed process is fundamentally different from the state-of-the-art that realises power generation from LOHC-bound hydrogen in a sequence of endothermal H18-DBT dehydrogenation to produce hydrogen gas followed by hydrogen purification and use of the so-obtained pure hydrogen in a fuel cell. In contrast, we here propose a sequence that does not involve molecular hydrogen at any point. Instead, a reaction cascade is established that consists of a heterogeneously catalysed, almost thermoneutral transfer hydrogenation step converting acetone to 2-propanol by contacting H18-DBT, acetone and a catalyst at temperatures in the range of 150 to 190 °C. This step is followed by the direct digestion of 2-propanol in a PEMFC at 85 to 90 °C. Because acetone is the only detectable product of the oxidation of 2-propanol, it can be recycled to the transfer hydrogenation reactor. Thus, the 2-propanol/acetone reaction pair acts as an efficient hydrogen transfer system to activate the LOHC-bound hydrogen for the here-presented integrated fuel cell operation.

Our paper demonstrates all relevant steps of this new concept. Although there is clearly room for further improvement of the transfer hydrogenation and electrocatalytic oxidation step, the potential of the approach with respect to energy efficiency, power density and safety is clearly recognisable. Using Pt/C as standard transfer hydrogenation catalyst and PtRu/C as electrocatalyst at the fuel cell anode, the reaction sequence has been realised with up to 20 % of the power density otherwise obtained in the fuel cell with pure hydrogen. In addition, further development potential has already been identified via advanced electrochemical methods with coupled analytics. Further insights into the crucial acetone desorption will pave the way for a knowledge-driven optimisation of the anode catalyst material and overall fuel cell operation strategy.

Most importantly, the here presented sequence of transfer hydrogenation and fuel cell operation does not require an external heat input. The first step, the transfer hydrogenation from H18-DBT to acetone is very mildly exothermic as two C-H bonds in H18-DBT are replaced by one C-H-bond and one O-H-bond in 2-propanol. The second step, the conversion of 2-propanol in a PEMFC does not require external heat input as the endothermal release of protons from 2-propanol is overcompensated by the exothermal formation of water in the fuel cell. This is in sharp contrast to the classical sequence involving endothermal H18-DBT dehydrogenation, where 27 % of the Lower Heating Value (LHV) of the released hydrogen has to be introduced into the system to drive the LOHC dehydrogenation at a temperature level of 280 to 320 °C. This difference is highly relevant for the achievable BH2E efficiencies. Considering that both concepts could be used to power a vehicle, the classical

dehydrogenation/fuel cell-sequence has a potential for 32 to 38 % BH2E efficiency. In contrast, we have shown in this contribution a potential for over 50 % BH2E for our proposed transfer hydrogenation/fuel cell sequence. Due to this very remarkable increase in efficiency, we anticipate that our new concept will be of great interest if LOHC-bound hydrogen should be used to power vehicles or off-grid power devices.

Article Online
DOI: 10.1039/C9EE01324E

Acknowledgements

This project was financially supported by the DFG through the Erlangen Cluster of Excellence “Engineering of Advanced Materials” in the framework of the excellence initiative (Bridge Funding). G. S., D. G., T. S., P. P., and P.W. acknowledge additional financial support from the Free State of Bavaria through its institutional and project-based support for the HI ERN. The German Federal Ministry of Education and Research (BMBF) is gratefully acknowledged for sponsoring some of the initial work in transfer hydrogenation using LOHC-bound hydrogen through its Kopernikus project “Power2X”, in particular the LOHC-cluster B1.

References

View Article Online
DOI: 10.1039/C9EE01324E

- [1] D. Teichmann, W. Arlt, P. Wasserscheid and R. Freymann, *Energy Environ. Sci.*, 2011, **4**, 2767-2773.
- [2] P. Preuster, C. Papp and P. Wasserscheid, *Acc. Chem. Res.*, 2017, **50**, 74-85.
- [3] P. T. Aakko-Saska, C. Cook and J. Kiviaho, T. Repo, *J. Power Sources*, **396**, 803-823.
- [4] P. Preuster, A. Alekseev and P. Wasserscheid, *Ann. Rev. Chem. Biomol. Eng.*, 2017, **8**, 445-471.
- [5] N. Brückner, K. Obesser, A. Bösmann, D. Teichmann, W. Arlt, J. Dungs and P. Wasserscheid, *ChemSusChem*, 2014, **7**, 229-235.
- [6] H. Jorschick, P. Preuster, S. Dürr, A. Seidel, K. Müller, A. Bösmann and P. Wasserscheid, *Energy Environ. Sci.*, 2017, **10**, 1652-1659.
- [7] see, e.g. www.hydrogenious.net.
- [8] D. Teichmann, W. Arlt and P. Wasserscheid, *Int. J. Hydrogen Ener.*, 2012, **37**, 18118-18132.
- [9] M. Reuss, T. Grube, M. Robinius, P. Preuster, P. Wasserscheid and D. Stolten, *Appl. Ener.*, 2017, **200**, 290-302.
- [10] K. Müller, K. Stark, V. N. Emel'yanenko, M. A. Varfolomeev, D. H. Zaitsau, E. Shoifet, C. Schick, S. P. Verevkin and W. Arlt, *Ind. Eng. Chem. Res.*, 2015, **54**, 7967-7976.
- [11] U. Eberle, M. Felderhoff and F. Schüth, *Angew. Chem., Int. Ed.*, 2009, **48**, 6608-6630.
- [12] P. Preuster, Q. Fang, R. Peters, R. Deja, V. N. Nguyen, L. Blum, D. Stolten and P. Wasserscheid, *Int. J. Hydrogen Ener.* 2018, **43**, 1758-1768.
- [13] G. Wang, Y. Yu, H. Liu, C. Gong, S. Wen, X. Wang and Z. Tu, *Fuel Process. Technol.*, 2018, **179**, 203-228
- [14] D. Stolten and B. Emons (eds.), "Hydrogen Science and Engineering", Wiley-VCH, Weinheim, 2016 (ISBN: 978-3-527-33238-0).
- [15] D. Cao and S. H. Bergens, *J. Power Sources*, 2003, **124**, 12-17.
- [16] Z. Qi, M. Hollett, A. Attia and A. Kaufmann, *Electrochem. Solid St.*, 2002, **5**, A129-A130.
- [17] Z. Qi and A. Kaufmann, *J. Power Sources*, 2002, **112**, 121-129.
- [18] S. Sen Gupta and J. Datta, *J. Chem. Sci.*, 2005, **117**, 4, 337-344.
- [19] C. Lamy, A. Lima, V. LeRhun, F. Delime, C. Coutanceau, and J-M. Léger, *J. Power Sources*, 2002, **105**, 2, 283-296.
- [20] S. Wasmus and A. Küver, *J. Electroanal. Chem.*, 1999, **461** (1), 14-31.
- [21] P. Driscoll, E. Deunf, L. Rubin, O. Luca, R. Crabtree, C. Chidsey, J. Arnold, and J. Kerr, *ECS Trans.* 2011, **35** (28), 3-17.
- [22] J. R. Ferrell, S. Sachdeva, T. A. Strobel, G. Gopalakrishnan, C. A. Koh, G. Pez, A. C. Cooper and A. M. Herring, *J. Electrochem. Soc.* 2012, **159** (4), B371-B377.
- [23] <https://www.balticfuelcells.de/liquidCoolE.html>, last assessed 20th of April 2019.

- [24] A. K. Schuppert, A. A. Topalov, I. Katsounaros, S. O. Klemm and K. J. J. Mayrhofer, *J. Electrochem. Soc.*, 2012, **159**, F670-F675. [View Article Online](#)
DOI: 10.1039/C9EE01324E
- [25] P. Khanipour, M. Löffler, A. M. Reichert, F. T. Haase, K. J. J. Mayrhofer, I. Katsounaros, *Angew. Chem. Int. Ed.*, accepted manuscript, DOI: 10.1002/anie.201901923.
- [26] P. Kurzweil in *Brennstoffzellentechnik* 145–162 (Springer Fachmedien, 2016).
doi:10.1007/978-3-658-14935-2.
- [27] X.-Z. Yuan, S. Zhang, H. Wang, J. Wu, J. C. Sun, R. Hiesgen, K. A. Friedrich, M. Schulze, A. Haug, *J. Power Sources*, 2010, **195**, 22, 7594-7599.
- [28] M. S. Wilson, S. Gottesfeld, *J. Appl. Electrochemistry*, 1992, **22(1)**, 1-7.
- [29] G. Dellepiane, and J. Overend, *Spectrochimica Acta*, 1966, **22**, 593-614.
- [30] E. Pastor, S. González, A. J. Arvia, *J. Electroanal. Chem.* 1995, **395**, 233-242.